Maternal cold inducible RNA binding protein is required for embryonic kidney formation in *Xenopus laevis*

Ying Peng[a,1], K.H. Kok[b,e,1], Ren-He Xu[c], K.H.H. Kwok[e], David Tay[d], P.C.W. Fung[b], Hsiang-fu Kung[e], Marie C.M. Lin[e,*]

[a] *Department of Neurology, The First Military Medical University of China, Guangzhou, PR China*
[b] *Division of Medical Physics, Department of Medicine, The University of Hong Kong, Hong Kong, PR China*
[c] *WiCell Research Institute, 614 Walnut St., Madison, WI, USA*
[d] *Department of Anatomy, The University of Hong Kong, Hong Kong, PR China*
[e] *Institute of Molecular Biology, The University of Hong Kong, 8/F Kadoorie Biological Science Bldg., Pokfulam Rd, Hong Kong, PR China*

Received 30 June 2000; revised 21 August 2000; accepted 21 August 2000

Edited by Giulio Superti-Furga

Abstract We cloned a major isoform of *Xenopus* homologue of cold inducible RNA binding protein (CIRP), XCIRP-1. XCIRP-1 was neither cold inducible nor essential for cell division during early embryonic development. Suppression of XCIRP-1 dose dependently produced tailbuds with deformations of the brain and internal organs. The defects were XCIRP-1 specific as they could be rescued by sense transcript. Suppression of XCIRP-1 also disrupted the morphogenetic migration of the C3 blastomeres (lineaged to become the embryonic kidney, the pronephros). In animal cap explants, depletion of XCIRP-1 inhibited activin/retinoic acid induced expressions of pronephros related Xlim-1 and WT1 genes. These results suggest that XCIRP-1 is required for the specification and morphogenetic lineage migration of the pronephros.

Key words: Cold inducible RNA binding protein; cDNA cloning; Pronephros; Morphogenetic movement; *Xenopus laevis*

1. Introduction

RNA binding proteins mediate a diverse array of cellular processes including RNA translation [1], processing [2], transport [3], localization [4], storage [5] and stability [6]. A family of RNA binding proteins consisting of an N-terminal consensus sequence RNA binding domain and a C-terminal glycine-rich domain has been identified from many organisms including cyanobacterium [7], plants [8,9], and mammals [10]. The cold inducible RNA binding proteins (CIRP) from human [11], mouse [12], rat [13], Mexican axolot1 [14], *Xenopus* [15], and bullfrogs [16] belong to this family. In human and mouse cultured cells and in male germ cells, CIRP mRNA is induced by cold and depressed by heat stress, and it mediates the cold induced growth suppression presumably through prolonging the G1 phase of the cell cycle [17,18]. In the adult rat and *Xenopus*, CIRP mRNA level is cold inducible in the brain but not in the liver [13,16,18]. These multiple and tissue specific regulations together with their ubiquitous expression pattern in adult tissues imply that CIRP has diverse and tissue specific physiological functions.

The role of CIRP during embryonic development is not understood. In amphibians, CIRP is present in oocyte, its expression increased rapidly during gastrulation and later localized in neural tissues and the presumptive pronephros (embryonic kidney), suggesting that CIRP may play a role in neurogenesis and pronephrogenesis [14,15]. Vertebrates use a succession of different kidney forms to control water loss and excrete waste through embryonic and adult life. These kidney forms, the pronephros, mesonephros and metanephros, develop from intermediate mesoderm following a precise temporal and spatial sequence. Each kidney is formed as a result of an inductive interaction with the previous form. In amphibian, the pronephros is the fully functional embryonic kidney (reviewed in [19] and references therein). The pronephros differentiates from a part of the lateral mesoderm, and its development involves mesoderm induction, pattern specification, and morphogenetic movements. The mechanisms and factors specifying or regulating the pronephrogenesis are not well understood.

To explore the functional role of CIRP in vertebrate embryonic development particularly in kidney formation, we cloned a major form of *Xenopus* homologue of CIRP, XCIRP-1. Our clone differs from that of the reported XCIRP in its abundance and the 3′ end nucleotide and amino acid sequences. By loss of function studies, we showed that XCIRP-1 is essential for embryonic development and the formation of the pronephros. Although several RNA binding proteins are expressed in kidney during embryonic development, their functions in kidney development are not clear. To our knowledge, this is the first evidence demonstrating the requirement of a maternal RNA binding protein in the specification and morphogenetic lineage migration of the embryonic kidney, the pronephros.

2. Materials and methods

2.1. Cloning a major form of Xenopus laevis homologue of cold inducible RNA binding protein (XCIRP-1)

The developmental stages of *Xenopus* embryos were determined

*Corresponding author. Fax: (85)-2-28171006.
E-mail: mcllin@hkusua.hku.hk

[1] These authors contributed equally to the manuscript.

Abbreviations: CIRP, cold inducible RNA binding protein; RA, retinoic acid; Xlim-1, LIM class homeobox containing gene; WT1, Wilm's tumor suppressor gene; Xbra, *Xenopus* brachyury; EF-1α, elongation factor-1 α; AC, animal cap

0014-5793/00/$20.00
PII: S0014-5793(00)02019-6

according to that described by Nieuwkoop and Faber [20]. One μg of poly(A+) RNA isolated from stage 17 embryos was used to prepare the adapter ligated double-strand (ds) cDNA library according to the procedure described in the Marathon cDNA Amplification Kit (Clontech, Palo Alto, CA, USA). *Xenopus* homologue of CIRP was cloned by reverse transcription (RT) and polymerase chain reaction (PCR) using primers designed from the conserved human nucleotide sequences encoding the two RNA binding domains (sense primer: 5′-AAACTTTTTGTTGGAGGGCTGA-3′; antisense primer: 5′-TCTCAAAGGTGACAAACCCAAA-3′). The 3′ and 5′ ends of XCIRP-1 were amplified from the library using the flanking adapter specific primer AP1 (supplied by the manufacturer) paired with a sense and an antisense primer, respectively, designed from the amplified cDNA sequences. The full length cDNA was obtained by a PCR reaction using primers designed from the most 5′ and 3′ end sequences (sense primer: 5′-TGAATTCTTTGACGAGCAGC-3′; antisense primer: 5′-TAATAGGCTTCGTGAAGCCA-3′). The full length PCR products (1.3 kb) from five separate reactions were combined and subcloned into pCR2.1. Plasmids of both sense and antisense orientations were isolated. The consensus cDNA nucleotide sequences of three randomly chosen clones were obtained and found to be highly homologous to the reported human, mouse, rat, Mexican axolot1, bullfrog, and *Xenopus* CIRPs.

2.2. RT-PCR

Total RNA was extracted from embryos and adult tissues with Trizol reagent (GIBCO Bethesda Research Lab.) in accordance with the manufacturer's instructions. RT-PCR was performed using the Superscript Preamplification System (GIBCO Bethesda Research Lab.). Primer sets and PCR conditions for EF-1α [21], Xbra [22], muscle actin [23], Xlim-1 [24] and WT1 [25] have already been described. PCR condition for XCIRP-1 and the reported XCIRP was as follows: 30 s at 98°C, 1 min at 57°C, 1 min at 72°C for 27 cycles. We used a common sense primer for both XCIRP isoforms: F198, 5′-GTTGATGATGCCAAGGATGC-3′ (nt 198–217). XCIRP-1 specific antisense primers are R532, 5′-TACTCGTGTGTAGCATAG-3′ (nt 532–525) and R794, 5′-CAGCCCAAATGGAACAGC-3′ (nt 794–777). XCIRP specific antisense primers are R′535, 5′-TGCATCTAGTCAGCCATA-3′ (nt 535–518) and R′794, 5′-CGAATCAGGCGTTTCCA-3′ (nt 794–777). Although data are shown from individual experiments, in all cases multiple PCR cycles were conducted to first determine the proper cycle number and the results were confirmed in multiple independent trials.

2.3. RNA preparation and embryo micro-injection

The sense and antisense capped mRNAs were synthesized from linearized plasmid constructs by in vitro synthesis using a transcription kit (Ambion). The synthetic RNA was quantitated by ethidium bromide staining in comparison with a standard RNA and by the spectrophotometric determination. Embryos were obtained by in vitro fertilization and micro-injections were performed as previously described [23].

2.4. Whole-mount X-gal staining and histology

β-Gal expressing embryos were collected at appropriate stages, fixed, and stained for the presence of β-gal with X-gal by standard staining technique. For histological analysis, the above β-gal expressing embryos were fixed in 2% paraformaldehyde, dehydrated, embedded in paraffin. The embryos were sectioned horizontally through the head and pronephros, and stained with hematoxylin and eosin.

3. Results

3.1. Nucleotide and amino acid sequences, relative abundance, and expression patterns of XCIRP-1

The CIRP isolated in this study was named XCIRP-1 (nt = 1241 bp, amino acid residues = 166) to distinguish it from a previously reported XCIRP (nt = 887 bp, amino acid residues = 163) [15]. The deduced amino acid of XCIRP-1 (GenBank accession number BankIt341921 AF278702) is highly homologous to all of the reported CIRP proteins. The characteristic two RNA binding domains and the glycine-rich C-terminal domain are well conserved among all. XCIRP-1 differs from that of the reported XCIRP at one amino acid in the N-terminal region, and contains four additional amino acids in the C-terminal end, which are also conserved in the human, mouse, and rat proteins. The major difference of the two *Xenopus* CIRP clones lies in the 3′

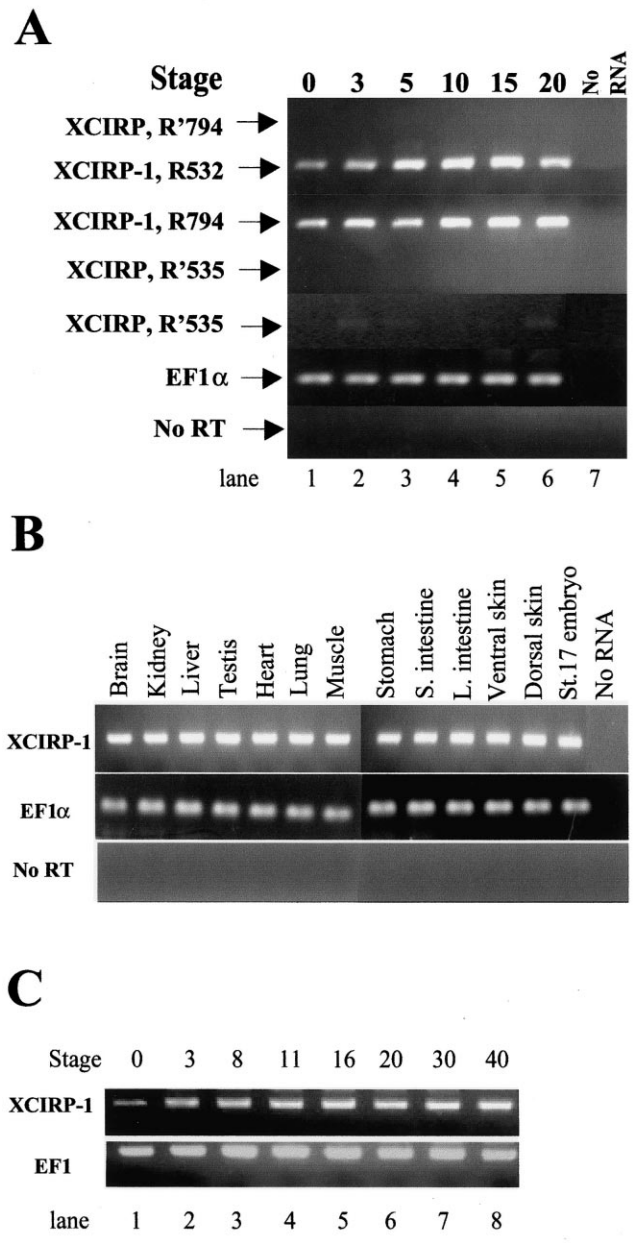

Fig. 1. Gene expression patterns of XCIRP-1. The levels of XCIRP-1 mRNA were determined by RT-PCR as indicated in Section 2, using total RNA as template. Tissues or embryos processed for RT-PCR in the absence of reverse transcriptase (No RT) were used as negative control. XEF-1a served as a loading control mRNA. Unless specified, XCIRP-1 mRNA level was determined using primer pairs F198 and the XCIRP-1 specific R794, PCR cycle = 27. A: The relative levels of XCIRP-1 and XCIRP mRNA were determined by competitive RT-PCR using a common sense primer F198 paired with two pairs of gene specific antisense primers as indicated. B: Tissue distribution of XCIRP-1 mRNA was determined using total cellular RNA isolated from various tissues of a male adult frog. C: Total RNA isolated from mature oocytes or embryos at different developmental stages were used as the template.

non-coding region, where no significant sequence homology was found. The 3′ end nucleotide sequence of XCIRP-1 is highly homologous (89%) to that of a *Xenopus* 3′ end cDNA fragment 5G10 [26] recently isolated by a large-scale gene expression screen.

To determine the relative abundance of XCIRP-1 and XCIRP, we designed two gene specific antisense primers for each cDNA: R532 and R794 for XCIRP-1; and R′535 and R′794 for XCIRP [15]. Two competitive RT-PCR reactions were conducted using a common sense primer (F198) paired with two antisense primers, one from each cDNA to generate PCR products of different sizes. As shown in Fig. 1A, only XCIRP-1 specific PCR product was obtained from oocytes or embryos of various developmental stages (stages 3–20). In addition, under the same condition, only low level of PCR product was detectable using F198 and a XCIRP specific antisense primer. These results indicate that XCIRP-1 is the predominant isoform.

The gene expression pattern of XCIRP-1 in various adult tissues of a male *Xenopus* was investigated by RT-PCR. XCIRP-1 mRNA was detected in all of the following 12 tissues we examined: kidney, brain, lung, liver, heart, muscle, testis, stomach, small intestine, large intestine, dorsal and ventral skins (Fig. 1B). This is consistent with the finding in mouse and human cell lines [11,12], in adult rat [13] and Mexican axolot1 [14]. The temporal and spatial gene expression patterns of XCIRP-1 during embryonic development were determined and found to be identical to that reported for XCIRP [15]. XCIRP-1 transcript is present at low level in the mature oocyte, the expression level increases significantly after fertilization, and is maintained high throughout organogenesis (Fig. 1C). It is expressed in the animal half of the embryo, then the neural crest and neural tube in neurula stages, and finally in the neural tissues and pronephros region in tailbud stage (not shown).

3.2. Phylogenetic analysis, cell cycle control, and cold inducibility

To understand the genetic relationship of CIRP and other RNA binding proteins, we constructed a phylogenetic tree. Phylogenetic analysis of the amino acid sequences (Fig. 2A) shows that XCIRP-1 has close evolutionary relationship to a family of mammalian RNA binding proteins (RBM and RNBP) which play a role in spermatogenesis. XCIRP-1 is also evolutionarily related to the plant glycine-rich RNA binding proteins. Some members of this plant protein family (GRP, GRP2, and whGRP-1) have been shown to participate in regulating RNA transcription and processing during cold stress. Others (GRP1A, GRP1) have been shown to play a general role in circadian phenomena associated with meristematic tissue. Such analysis is consistent with the expression of XCIRP-1 in the sperm and the reports that in cell lines and/or in adult brain tissues, CIRPs are cold inducible, depressed by heat or oxidative stress, may participate in cell cycle control and are circadian regulated.

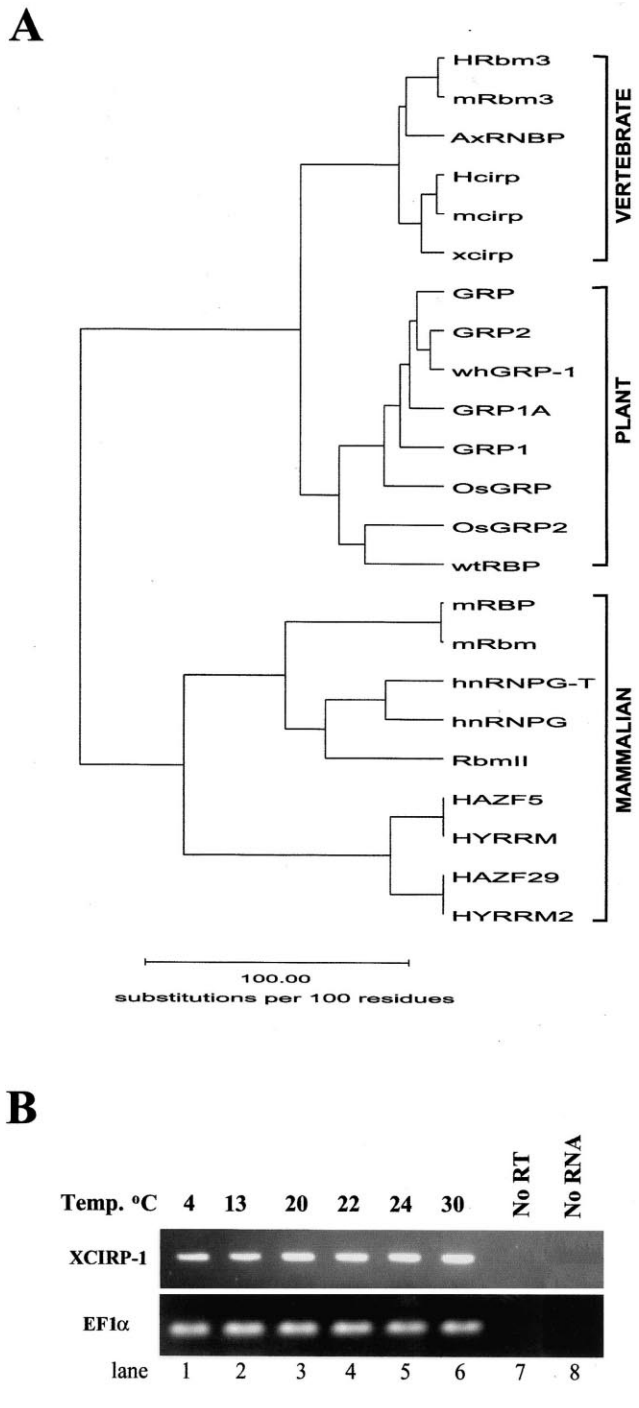

→

Fig. 2. Phylogenetic tree of the CIRP family and the effects of cold and heat stress on XCIRP-1 expression. A: Amino acid sequences analyzed in this study were retrieved from public electronic databases: HRbm3, mRbm3, and AxRNBP: human, mouse, and Ambystoma mexicanum [20] RNA-binding proteins; Hcirp, mcirp, xcirp: human, mouse, and *Xenopus* cold inducible RNA binding proteins; GRP, GRP2, whGRP-1, GRP1A, GRP1, OsGRP, and OsGRP2: carrot, sorghum, wheat, white mustard, Pelargonium hortorum, and Oryza sativa (rice) glycine-rich RNA binding proteins; wtRBP: wood tobacco RNA binding protein; mRBP and mRbm: mouse RNA binding proteins; hnRNPG and hnRNPG-T: human heterogeneous and testes specific nuclear ribonucleoprotein G; HAZF and HYRRM: human spermatogenesis factor AZF and Y-chromosome RNA recognition motif protein. The phylogeny was derived by the UPGMA method applied to pairwise sequence distances calculated using the Kimura protein method. B: Effects of cold and heat stress on XCIRP-1 mRNA level were determined by RT-PCR as described in Section 2 and in Fig. 1. Total RNA was isolated from stage 9 embryos cultured at 4, 13, 22, 24, and 30°C for 4 h.

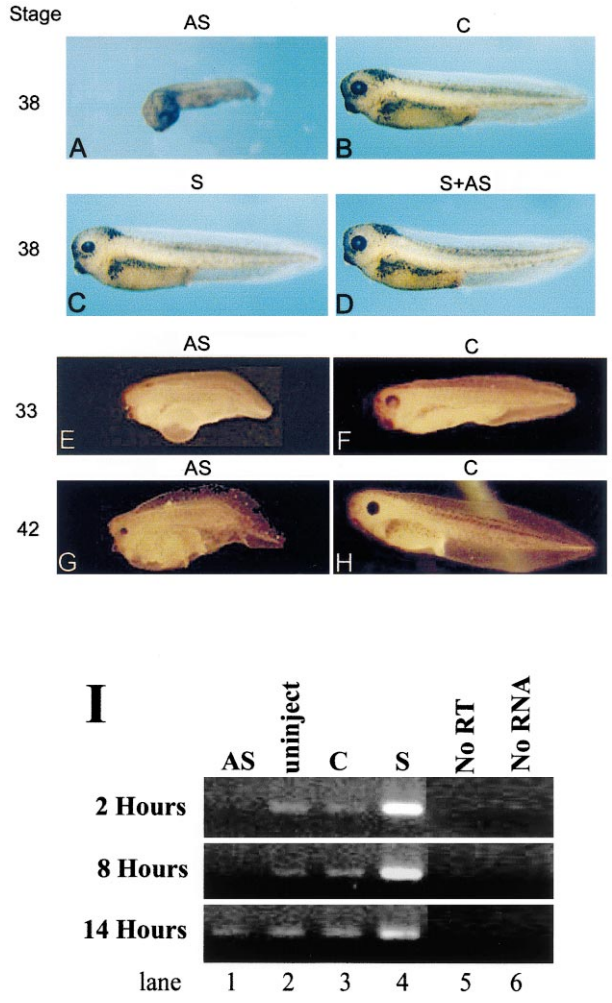

Fig. 3. Suppression of XCIRP-1 results in dose dependent deformations of the embryos. The two blastomeres of the two-cell stage embryos were injected with 1 ng (A–D), or 0.5 ng (E–H) of antisense (AS), sense (S), S+AS XCIRP-1 transcripts or equal amount of β-gal mRNA (control, C), and allowed to develop to various stages as indicated on the left column. I: Two-cell stage embryos were injected with 2 ng of antisense (AS), sense (S) XCIRP-1 or β-gal (C) mRNA. They were allowed to grow for the time (h) indicated, and the effects of injections on XCIRP-1 mRNA level were determined by RT-PCR as described in Section 2 and Fig. 1.

To test the effect of XCIRP-1 in embryonic cell division/cell cycle control, we injected 3, 2, 1, and 0.5 ng of sense or antisense XCIRP-1 into one of the two cells in two-cell stage embryos (15–20 embryos per group). The effect on cell division in embryo was observed continuously from developmental stage 2 to stage 9 (approximately for 5 h), using the uninjected side as control. Surprisingly, neither sense nor antisense XCIRP-1 transcript caused any effect on the rate of cell division (data not shown) suggesting that XCIRP-1 is dispensable in embryonic cell division/cell cycle control.

The effects of cold and heat stress on XCIRP-1 mRNA level in *Xenopus* embryo were investigated by culturing stage 9 embryos at 4, 13, 22, 24, and 30°C for 4 h. At the end of incubation, the levels of XCIRP-1 mRNA were determined by RT-PCR. Again, to our surprise, in all cases, the levels of XCIRP-1 mRNA were unchanged (Fig. 2B). In another experiment, stage 4 embryos were exposed to cold stress at 13°C for up to 24 h and XCIRP-1 mRNA levels were determined at 4, 8, 18, and 24 h post cold shock and compared to that of stage matched control embryos maintained at room temperature. Again, no change was observed (data not shown). This is contrary to the results obtained in cell lines and in adult brain tissues. Therefore, it raises the possibility that the cell cycle control and cold inducibility are acquired later in life in a tissue specific manner.

3.3. *Suppression of maternal XCIRP-1 gene expression produced multiple defects in the brain and internal organs*

To understand the role of XCIRP-1 during embryonic development, we injected various doses of sense or antisense XCIRP-1 into the two blastomeres of the two-cell stage embryos and observed the resultant phenotypes (Table 1). Blocking XCIRP-1 expression by antisense XCIRP-1 transcript did not produce detectable alternation in either the morphology or the rate of embryonic development before the embryos reach late neurula/initial organogenesis stages. However, after the beginning of organogenesis (around stage 22), antisense XCIRP-1 dose dependently caused embryonic malformations (Table 1 and Fig. 3A,E,G). One ng of antisense XCIRP-1 resulted in 56% death and death occurred at around stage 22. The surviving tadpoles were able to develop to around stage 38–40 with severe deformations particularly of the brain and internal organs (Fig. 3A) as compared to the control β-gal injected embryos (Fig. 3B). The defects were XCIRP-1 specific, as the full length sense XCIRP-1 can rescue these

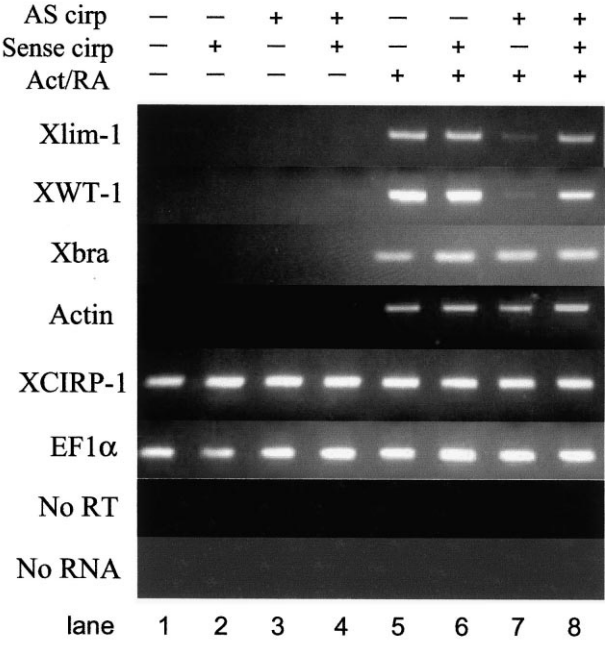

Fig. 4. Effect of XCIRP-1 on the expressions of activin/RA induced mesoderm and pronephros related genes. Embryos were injected with 2 ng of RNA encoding β-gal, sense XCIRP-1, antisense XCIRP-1, or sense plus antisense XCIRP-1 to the two cells of the two-cell stage embryos. The blastula stage animal caps were dissected at stage 8.5 and cultured in buffer containing activin (10 ng/ml) and RA (10^{-5} M) until sibling controls reached stage 28–30 (tailbud stage). RNAs were extracted and mRNA levels were determined by RT-PCR (see Section 2). The EF-1α mRNA level was used as a loading control and embryos processed for RT-PCR in the absence of reverse transcriptase (No RT) was used as a negative control.

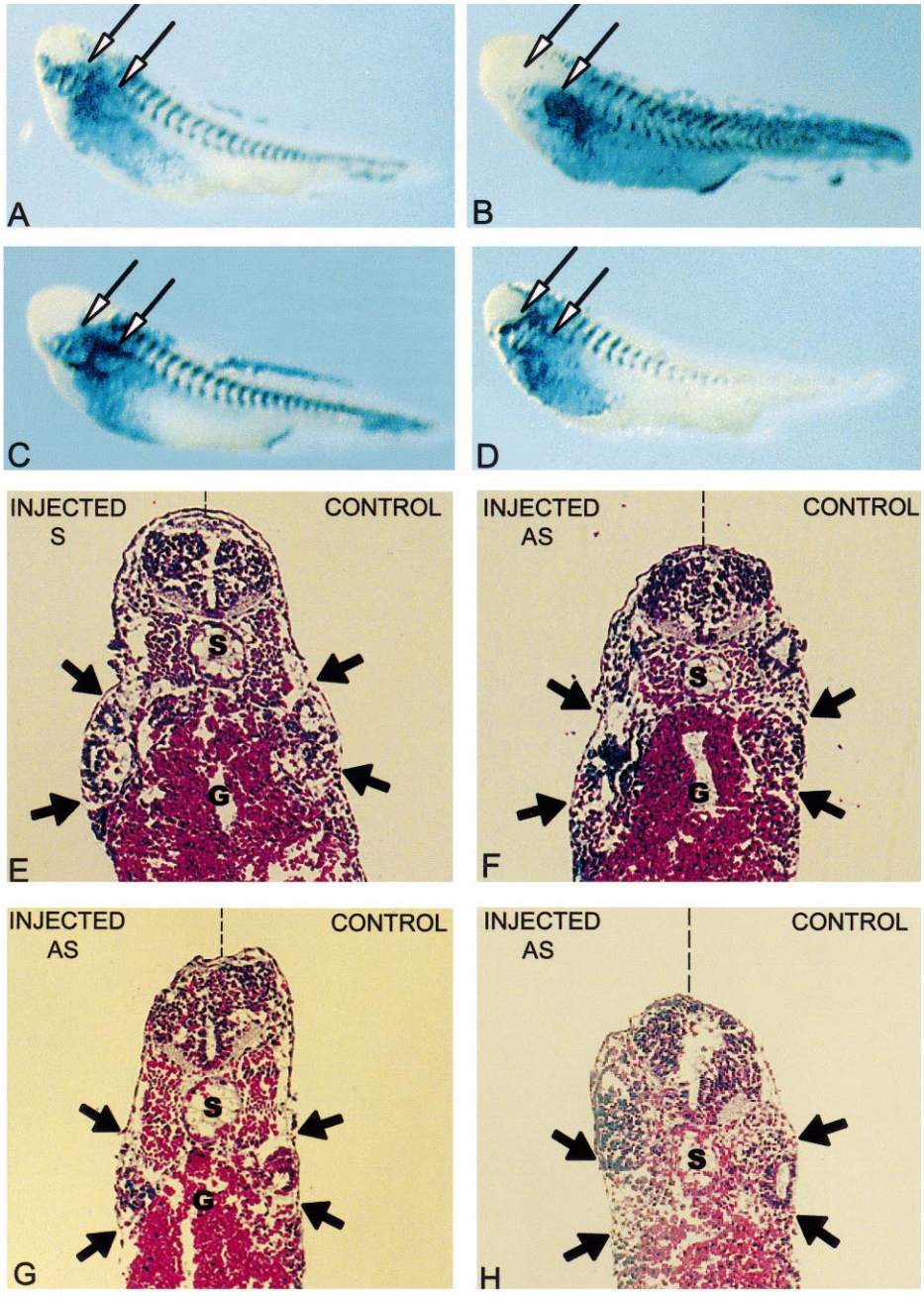

Fig. 5. Effect of XCIRP-1 on the morphogenetic lineage migration of C3 blastomeres and pronephros formation. The morphogenetic lineage migration of C3 blastomeres was examined by injecting to one of the C3 blastomeres (at 32-cell stage) with the following mRNAs. A: 0.05 ng of β-galactosidase (β-gal); B: β-gal with 0.2 ng of antisense XCIRP-1; C: β-gal with 0.2 ng of sense XCIRP-1; and D: β-gal with 0.2 ng each of antisense and sense XCIRP-1. The embryos were then allowed to develop until the tailbud stage (stage 28–30), fixed and stained. The morphogenetic migration pattern of the C3 blastomeres was visualized by X-gal whole-mount staining. In addition, the pronephros formation was also examined by the histological analysis of the mid-dorsal section of the stage 28–30 tailbuds which were injected at one of the C3 cells with E: 0.2 ng of sense XCIRP-1 and F–H: 0.2 ng of antisense XCIRP-1.

multiple defects (Fig. 3D). Forced overexpression of sense transcript alone did not cause any deformation (Fig. 3C). Injection of 0.5 ng of antisense XCIRP-1 produced tailbuds (Fig. 3E, stage 33) with edema of the internal organs and tadpoles (Fig. 3G, stage 42) with defects including malformation of the brain and internal organs. Again, co-injection of full length sense RNA can fully rescue these defects, the morphology of the embryos is indistinguishable from that of the control (Fig. 3F,H). Injection of 0.25 ng of antisense XCIRP-1 did not produce any phenotype (Table 1). RT-PCR analysis confirmed that injection of 2 ng of antisense XCIRP-1 caused significant suppression of the XCIRP-1 mRNA level for approximately 8 h, before the onset of mid-blastula transition stage (Fig. 3I). These results suggest that maternal XCIRP-1 plays an essential role in the specification of multiple organs, which may include kidney.

Table 1
Abnormal phenotype induced by XCIRP-1 transcripts[a]

Injection samples	No. of embryos	Normal	Defect. phenotype[b]	Dead
1 ng β-gal RNA	99	92% (91)	0% (0)	8% (8)
1 ng AS RNA	105	11% (11)	33% (35)	56% (59)
1 ng AS RNA+1 ng S RNA	99	70% (70)	10% (10)	20% (20)
1 ng S RNA	85	93% (79)	0% (0)	7% (6)
0.5 ng AS RNA	82	35% (29)	48% (39)	17% (14)
0.25 ng AS RNA	75	77% (58)	0% (0)	23% (17)

[a]Values are the combined data of 5–6 independent experiments with each experiment consisting of 10–20 embryos. Bracketed figures indicate the number of embryos with the specified phenotype.
[b]Defective phenotypes include malformations of the brain and the internal organs.

3.4. Depletion of maternal XCIRP-1 mRNA specifically inhibited the expressions of pronephros related Xlim-1 and WT1 genes

XCIRP has been suggested to be a candidate pronephrogenesis related gene [15]. As the pronephros is developed from the lateral plate mesoderm and activin (10 ng/ml)/RA (10^{-5} M) have been shown to cause both the mesoderm and pronephric tubules induction [27], we tested the effects of XCIRP-1 on activin/RA stimulated mesoderm and pronephros induction in animal cap (AC) explants. Embryos were injected with 2 ng of sense and/or antisense XCIRP-1 transcripts at two-cell stage, the ACs were obtained at stage 8.5–9, cultured in the presence and absence of activin/RA until stages 11, 20 or 28–30. The morphologies of the ACs were recorded and then they were harvested for RNA analysis by RT-PCR. Neither sense nor antisense XCIRP-1 transcript had any effect on activin/RA induced mesoderm elongation of the AC explants (data not shown). This is consistent with their lack of effect on the expression of the general mesoderm markers, muscle actin and Xbra (data not shown), suggesting that XCIRP-1 does not affect general mesoderm induction.

To investigate the effect of XCIRP-1 on activin/RA induced expressions of the pronephros related genes, we determined the expressions of Xlim-1 and WT1 genes. AC explant studies were conducted as described above, and the explants were harvested at stage 28–30 for RNA analysis. While sense XCIRP-1 had no effect, antisense XCIRP-1 inhibited the expressions of Xlim-1 and XWT1 genes. Whereas the expressions of muscle actin and Xbra and EF1-α genes were not affected (Fig. 4). These inhibitions could be rescued by the full length sense transcript. Taken together, these results suggest that XCIRP-1 is required for the specification of the pronephros rather than on the early induction of the mesoderm.

3.5. Depletion of maternal XCIRP-1 changed the morphogenetic lineage migration of C3 blastomeres and prevented pronephros formation

In addition to mesoderm induction and pattern formation, embryonic kidney development also involves morphogenetic movements. Therefore, we investigate the effect of XCIRP-1 in the migration and differentiation of the C3 blastomeres (lineaged to become pronephros). We injected sense, antisense, or combined sense/antisense CIRP transcripts with a tracer RNA encoding β-galactosidase (β-gal) to one of the C3 blastomeres at 32-cell stage embryos. The C3 blastomeres have been shown [28] to become the somite (42%), lateral plate including pronephros (20%), endoderm (17%), epidermis (9%), trunk mesenchyme (3%), and anterior mesoderm (3%). The migrations of the C3 blastomeres were determined at the tailbud stage (stage 30) by X-gal whole-mount staining of the tracer β-gal. As expected, the X-gal stain distributed proportionally in all of the corresponding tissues in control tailbud injected with β-gal alone (Fig. 5A). However, tailbuds injected with antisense XCIRP-1 had X-gal stain accumulated around and immediately below the pronephros region (between two arrows indicating the locations of somites 3 and 7) and on the epidermis (Fig. 5B). This aberrant staining pattern could be fully rescued by the sense XCIRP-1 transcript (Fig. 5D). Sense XCIRP-1 alone did not change the distribution of the X-gal stain (Fig. 5C).

The first histological indication of pronephros development in *Xenopus* is observable at around stage 21 when cells begin to condense away from the intermediate mesoderm below somites 3 to 5 (head somites 3 and 4 and trunk somite 1). These cells will form the main body of the pronephros. At stage 25 the main body of the pronephros appears as a solid mass of cells immediately below somites 3 and 4. After stage 30 the pronephros begins to develop a lumen and branch into the pronephric tubules. We chose to examine the pronephros structure at stage 28–30. During this period the pronephric anlage is visible as aggregated cells arranged in a radial fashion located between somites 3–7 which can be identified without much difficulty (see [29] for full description). Histological examination of multiple serial sections through the mid-dorsal region of the embryos (three embryos per group) clearly showed that in all cases, the pronephros structure (located between two arrows) was defective in the sides injected with antisense XCIRP-1 transcript, whereas un-injected control sides were normal (Fig. 5F,G,H). On the contrary, sense XCIRP-1 did not affect the normal development of the pronephros structure (Fig. 5E).

4. Discussion

Emerging evidence strongly suggests that CIRP plays diverse and tissue specific roles in adult animals. In this study, we cloned a major form of *Xenopus* CIRP, XCIRP-1 and further showed that maternal XCIRP-1 is required for the formation of embryonic kidney. We showed that suppression of XCIRP-1 in the C3 blastomeres altered the morphogenetic lineage movement of the C3 cells and resulted in a defective pronephros structure in tailbud. In accordance with these observations, in AC explant studies, depletion of XCIRP-1 mRNA by ectopic injection of antisense XCIRP-1 transcript at two-cell stage inhibited activin/RA induced expression of the Xlim-1 gene and XWT1 gene at tail bud stage. Furthermore, all of these inhibitory effects were fully rescued by the sense transcript, indicating that the above-mentioned effects

are specific for XCIRP-1. The expression of XCIRP-1 in the pronephros region during tailbud stage is also consistent with its role in embryonic kidney development. It is noteworthy, however, that forced overexpression of XCIRP-1 had no effect on any of the above-mentioned phenomena, suggesting that XCIRP-1 is not a morphogen, and that its level is not limiting.

WT1 encodes a transcription factor whose mutations are associated with both the renal Wilm's tumor and urogenital malformations [25]. Targeted mutation of WT1 results in renal aplasia in mouse [30]. Further studies showed that WT1 deficient mice are defected in the development of the caudal mesonephric tubules [31]. However, in amphibian, injection of *Xenopus* WT1 mRNA at early stage has been shown to inhibit pronephric tubules development [32]. This controversy may be due to an untimely disturbance of pronephros patterning, which may lead to non-physiological consequences. Our observation that antisense XCIRP-1 suppressed XWT1 expression accompanied by a defect in pronephros formation is consistent with the loss-of-function results derived from the mice study, and may represent a more physiological situation.

The expression and function of Xlim-1 are more complex. Xlim-1 plays a pivotal role during early ventrodorsal patterning of the mesoderm as well as the ectoderm [33,34]. Its later expression in lateral mesoderm begins at late gastrulation, and converges to the pronephros at tailbud stages. Xlim-1 expression precedes morphogenesis, suggesting that it may be involved in cell specification in these lineages. This raises the possibility that XCIRP-1 mediated Xlim-1 expression plays a critical role in the specification and migration of the pronephros cells. There is also evidence suggesting that Xlim-1 is involved in the anterior migration of the neural cells. Therefore, it may also contribute to the observed deformation of the brain (Fig. 3). The role of XCIRP-1 in neural development is complex and requires further investigation.

The underlying molecular mechanisms by which maternal XCIRP-1 exerts its effects are still not understood. It is possible that XCIRP-1 may have a general role in embryonic development. XCIRP-1 protein may be required for marking genes or gene transcripts for potential future activation. For example, it may change the conformation of RNA or DNA to establish competence to execute specific differentiation programs for organogenesis, with the actual activation being accomplished by stage/tissue specific signals. Future research is needed to discover the physiological processes and specific target RNAs regulated by XCIRP-1 protein. The relative simplicity of the *Xenopus* system would make it a very attractive model for explicating the roles and molecular mechanisms governing CIRP mediated embryonic development and organogenesis.

Acknowledgements: We wish to thank Dr. Dong-Yan Jin (Univ. of Hong Kong), Dr. Masanori Taira (Univ. of Tokyo), and Dr. Jaebong Kim (Hallym Univ., Korea) for discussions, suggestions and critical reading of this manuscript. We also wish to thank Miss Elsa Kao for technical assistance. The work described in this paper was supported by grants from the Research Grants Council of the Hong Kong Special Administrative Region, China (HKU 7166/99M and NSFC/HKU20 to H.f.K.). This work is also supported in part by grants from the Chinese National Nature Science Fund (39870267 to Y.P.), the HKU Central Allocation Fund (to P.C.W.F.), and a grant from The University of Hong Kong (to M.C.M.L.).

References

[1] Stripecke, R., Oliveira, C.C., McCarthy, J.E. and Hentze, M.W. (1994) Mol. Cell. Biol. 14, 5898–5909.
[2] Greenleaf, A.L. (1993) Trends Biochem. Sci. 18, 117–119.
[3] Michael, W.M., Siomi, H., Choi, M., Pinol-Roma, S., Nakielny, S., Liu, Q. and Dreyfuss, G. (1995) Cold Spring Harb. Symp. Quant. Biol. 60, 663–668.
[4] Ainger, K., Avossa, D., Diana, A.S., Barry, C., Barbarese, E. and Carson, J.H. (1997) J. Cell Biol. 138, 1077–1087.
[5] Curtis, D., Lehmann, R. and Zamore, P.D. (1995) Cell 81, 171–178.
[6] Sachs, A.B. (1993) Cell 74, 413–421.
[7] Sato, N. (1995) Nucleic Acids Res. 23, 2161–2167.
[8] Bergeron, D., Beauseigle, D. and Bellemare, G. (1993) Biochim. Biophys. Acta 1216, 123–125.
[9] Gomez, J., Sanchez-Martinez, D., Stiefel, V., Rigau, J., Puigdomenech, P. and Pages, M. (1988) Nature 334, 262–264.
[10] Derry, J.M., Kerns, J.A. and Francke, U. (1995) Hum. Mol. Genet. 4, 2307–2311.
[11] Nishiyama, H., Higashitsuji, H., Yokoi, H., Itoh, K., Danno, S., Matsuda, T. and Fujita, J. (1997) Gene 204, 115–120.
[12] Nishiyama, H., Itoh, K., Kaneko, Y., Kishishita, M., Yoshida, O. and Fujita, J. (1997) J. Cell Biol. 137, 899–908.
[13] Xue, J.H., Nonoguchi, K., Fukumoto, M., Sato, T., Nishiyama, H., Higashitsuji, H., Itoh, K. and Fujita, J. (1999) Free Radic. Biol. Med. 27, 1238–1244.
[14] Bhatia, R., Dube, D.K., Gaur, A., Robertson, D.R., Lemanski, S.L., McLean, M.D. and Lemanski, L.F. (1999) Cell Tissue Res. 297, 283–290.
[15] Uochi, T. and Asashima, M. (1998) Gene 211, 245–250.
[16] Saito, T., Sugimoto, K., Adachi, Y., Wu, Q. and Mori, K.J. (2000) Comp. Biochem. Physiol. B 125, 237–245.
[17] Nishiyama, H., Danno, S., Kaneko, Y., Itoh, K., Yokoi, H., Fukumoto, M., Okuno, H., Millan, J.L., Matsuda, T., Yoshida, O. and Fujita, J. (1998) Am. J. Pathol. 152, 289–296.
[18] Nishiyama, H., Xue, J.H., Sato, T., Fukuyama, H., Mizuno, N., Houtani, T., Sugimoto, T. and Fujita, J. (1998) Biochem. Biophys. Res. Commun. 245, 534–538.
[19] Vize, P.D., Seufert, D.W., Carroll, T.J. and Wallingford, J.B. (1997) Dev. Biol. 188, 189–204.
[20] Nieuwkoop, P.D. and Faber, J. (1967) Normal Table of Xenopus laevis (Daudin), North-Holland, Amsterdam.
[21] Krieg, P.A., Varnum, S.M., Wormington, W.M. and Melton, D.A. (1989) Dev. Biol. 133, 93–100.
[22] Smith, J.C., Price, B.M., Green, J.B., Weigel, D. and Herrmann, B.G. (1991) Cell 67, 79–87.
[23] Stutz, F. and Spohr, G. (1986) Mol. Biol. 187, 349–361.
[24] Xu, R.H., Kim, J., Taira, M., Zhan, S., Sredni, D. and Kung, H.F. (1995) Biochem. Biophys. Res. Commun. 212, 212–219.
[25] Semba, K., Saito-Ueno, R., Takayama, G. and Kondo, M. (1996) Gene 175, 167–172.
[26] Gawantka, V., Pollet, N., Delius, H., Vingron, M., Pfister, R., Nitsch, R., Blumenstock, C. and Niehrs, C. (1998) Mech. Dev. 77, 95–141.
[27] Moriya, N., Uchiyama, H. and Asashima, M. (1993) Dev. Growth Differ. 35, 123–128.
[28] Dale, L. and Slack, J.M.W. (1987) Development 99, 527–551.
[29] Nieuwkoop, P.D. and Faber, J. (1994) Normal Table of Xenopus laevis (Daudin), Garland, New York.
[30] Kreidberg, J.A., Sariola, H., Loring, J.M., Maeda, M., Pelletier, J., Housman, D. and Jaenisch, R. (1993) Cell 74, 679–691.
[31] Sainio, K., Hellstedt, P., Kreidberg, J.A., Saxen, L. and Sariola, H. (1997) Development 124, 1293–1299.
[32] Wallingford, J.B., Carroll, T.J. and Vize, P.D. (1998) Dev. Biol. 202, 103–112.
[33] Taira, M., Jamrich, M., Good, P.J. and Dawid, I.B. (1992) Genes Dev. 6, 356–366.
[34] Taira, M., Otani, H., Jamrich, M. and Dawid, I.B. (1994) Development 120, 1525–1536.